

## BIFURCATIONS OF PERIODIC SOLUTIONS AND CHAOS IN JOSEPHSON SYSTEM

ZHUJUN JING<sup>1,2</sup> K. Y. CHAN<sup>3</sup> DASHUN XU<sup>2</sup> HONGJUN CAO<sup>2</sup>

1. Dept. of Math., Hunan Normal University, Hunan Changsha, China.
2. Inst. of Math., Chinese Academy of Sciences, Beijing 100080, China.
3. Department of Mathematics University of Hong Kong.

(Communicated by Fanghua Lin)

**Abstract.** The Josephson equation is investigated in detail: the existence and bifurcations for harmonic and subharmonic solutions under small perturbations are obtained by using second-order averaging method and subharmonic Melnikov function, and the criterion of existence for chaos is proved by Melnikov analysis; the bifurcation curves about  $n$ -subharmonic and heteroclinic orbits and the driving frequency  $\omega$  effects to the forms of chaotic behaviors are given by numerical simulations.

**1. Introduction.** In this paper we consider the Josephson system

$$\begin{cases} \dot{x} = y \\ \dot{y} = -\sin x - k\sin 2x + \beta - \alpha(\cos x + 2k\cos 2x)y + f\sin\omega t. \end{cases} \quad (A)$$

Where  $x(t)$  is the phase-error process (i.e., an angular variable);  $\sin x + k\sin 2x$  is the Hybrid loop which represents the phase-detector characteristics;  $\omega$  and  $f$  are angular frequency and amplitude of the driving current (force) respectively;  $\sin\omega t$  represents a sinus plus noise;  $f\sin\omega t$  is a small sinusoidal force;  $-\alpha(\cos x + 2k\cos 2x)y + \beta$  is a characteristic of transfer functions of the ideal filter.

The domain of definition of the Josephson system is the tangent bundle of the circle  $\mathbf{TS}^1 = \mathbf{R}^2 \times \mathbf{S}^1$ , i.e., the cylinder. The detailed descriptive survey of Josephson System (A) may be found in [1, 3, 4, 11, 16]. The Josephson junction was first proposed by Josephson (see[18]), then the system has investigated by many authors, for example, see[1, 2, 4-15, 19-22, 24-29] and references there.

As is well known, the synchronous electric motor models of a single machine infinite bus [23], single point Josephson function [11], superconducting derive [8], forced pendulum [20, 25] and many other applications, can readily be described by the model, or analogous ones.

The study of Josephson system is of fundamental and even practical interest. On one the hand, the eminent characteristics of the Josephson system have a rich content of nonlinear properties which are suitable for a detailed investigating various dynamical states. On the other hand, an understanding of the dynamical behavior will be directly useful in the Josephson devices. We therefore think it is worthwhile to undertake a detailed discussion for the System (A) in order to point out which range of parameter corresponds to a certain behavior.

---

1991 *Mathematics Subject Classification.* 34C32, 35B32.

*Key words and phrases.* Josephson systems, bifurcations, periodic solution, chaos, second-order averaging and Melnikov methods.

This work is supported by the National Key Basic Research Fund (No. G1998020307) and the National Natural Science Foundation.

The dynamics of the forced Josephson junction circuit have been studied in the form of the equations

$$\begin{aligned}\beta\ddot{x} + \dot{x} + \sin x &= a + \epsilon \sin \omega t, \\ \dot{x} + \beta(1 + \alpha \cos x)\dot{x} + \sin x &= a + \epsilon \sin \omega t.\end{aligned}$$

in [1, 3, 9, 10, 25-29] and in other papers. These authors provided a qualitative analysis, given bifurcation diagrams, and investigated the chaotic states and the routes to chaos. In particular, they found the intermittent behavior (see[2, 8, 20, 34]), period-doubling bifurcations (see[7-9]), and period-triple bifurcations (see[8]) in such system.

The system in the form such as Josephson system (A) was less studied. In earlier papers [16, 17], we showed the existence of limit cycles and a saddle-to-saddle separatrix loop for  $f = 0$ , the existence of chaotic states for certain parameter regions using Melnikov method for  $f \neq 0$ . The chaos result from transverse intersection between the stable and unstable manifolds.

In this paper, the Eq.(A) is investigated in detail: the existence and bifurcations for harmonic and subharmonic solutions under small perturbations are obtained by using second-order averaging method and subharmonic Melnikov function, and the criterion of existence for chaos is proved by Melnikov analysis; the bifurcation curves about  $n$ -subharmonic and heteroclinic orbits are given by numerical simulations. We also present the driving frequency  $\omega$  effects to the forms of chaotic behaviors. In essence we use perturbation methods to study Eq.(A). We therefore introduce a small parameter  $\epsilon$ ,  $0 \leq \epsilon \ll 1$ , and assume that  $f = O(\epsilon)$ ,  $\alpha = O(1)$  or  $\alpha = O(\epsilon)$ , but  $k, \beta = O(1)$  or  $\beta = O(\epsilon)$  in Eq.(A). We will study how the dynamics of the unperturbed system are changed under the perturbation.

The paper is organized as follows. The bifurcations and classification of fixed points for unperturbed system are given in Section 2. Analytical results for the condition of existence and bifurcation of harmonics and subharmonics and the numerical simulations of bifurcations for the perturbed system are given in Section 3. In Section 4 Melnikov's method is used to prove the existence of "Smale-Birkhoff horseshoe" chaos, and the numerically investigation is considered to show some interesting attractors as the frequency  $\omega$  varies. In Section 5, we conclude with a summary and some comments.

## 2. Bifurcation and classification of fixed points for unperturbed system.

If  $\epsilon = 0$ , system (A) is considered as an unperturbed system and can be written as

$$\begin{cases} \dot{x} = y, \\ \dot{y} = -\sin x - k \sin 2x + \beta. \end{cases} \quad (2.1)$$

Eq.(2.1) corresponds to the non-damping, constant inputs case, and is a Hamiltonian system with a Hamiltonian function

$$H(x, y) = \frac{1}{2}y^2 - (\cos x + \frac{k}{2}\cos 2x) - \beta x. \quad (2.2)$$

Let

$$G(x) = -(\cos x + \frac{k}{2}\cos 2x) - \beta x. \quad (2.3)$$

The minima and maxima of  $G(x)$  correspond to the center and saddle-point of (2.1) respectively (see Fig.1). In Figure 2 we show the phase-portrait and heteroclinic orbits for  $k = 0.8, \beta = 0.001$ .

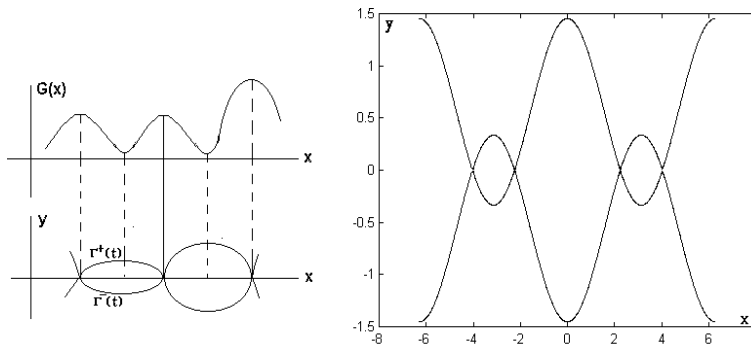


Figure 1

Figure 2

The fixed points of (2.1) satisfy the following equations:

$$\begin{cases} y = 0, \\ -\sin x - k\sin 2x + \beta = 0. \end{cases} \tag{2.4}$$

Let

$$F(x) = -(\sin x + k\sin 2x),$$

and  $\beta_1(k)$  and  $\beta_2(k)$  denote the maxima of  $F(x)$  as

$$\beta_1(k) = \frac{\sqrt{32k^2 - 2 + 2\sqrt{1 + 32k^2}}(\sqrt{1 + 32k^2} + 3)}{32k}, \tag{2.5}$$

and

$$\beta_2(k) = \frac{\sqrt{32k^2 - 2 - \sqrt{1 + 32k^2}}(\sqrt{1 + 32k^2} - 3)}{32k}. \tag{2.6}$$

The fixed point  $(x_j, 0)$  of (2.1) is a center if

$$\cos x_j + 2k\cos 2x_j > 0, \tag{2.7}$$

and a hyperbolic saddle if

$$\cos x_j + 2k\cos 2x_j < 0, \tag{2.8}$$

and a saddle-node point if

$$\cos x_j + 2k\cos 2x_j = 0. \tag{2.9}$$

Because the saddle-node bifurcation of a fixed point  $(x_j, 0)$  satisfies the conditions (2.4) and (2.9) simultaneously, we can prove that

$$\frac{\partial^2 F}{\partial x^2} \frac{\partial F}{\partial k} \Big|_{x=x_j, \beta=\beta_1(k) \text{ or } \beta=\beta_2(k)} = -(\sin x_j + 4k\sin 2x_j)(-\sin 2x_j) < 0. \tag{2.10}$$

Therefore, the saddle-node bifurcation is supercritical. By the above analysis it can be obtained without difficulty that

**Lemma 1** (i) For  $0 < \beta < \beta_2$  and  $k > \frac{1}{2}$ , there are four fixed points:  $(x_2, 0)$  and  $(x_4, 0)$  being saddle, and  $(x_1, 0)$  and  $(x_3, 0)$  being centers, where  $0 < x_1 < x_2 < \pi, \pi < x_3 < x_4 < 2\pi$  (see Fig.3).

(ii) For  $\beta_1 < \beta < \beta_2$  and  $k > \frac{1}{2}$  or  $0 < \beta < \beta_1$  and  $0 < k \leq \frac{1}{2}$ , there are two fixed points: center  $(x_1, 0)$  and saddle  $(x_2, 0)$  or center  $(x_3, 0)$  and saddle  $(x_4, 0)$ .

(iii) For  $\beta_1$  and  $\beta_2$  are saddle-node bifurcation values for fixed points: if  $\beta = \beta_1$  then there is a saddle-node  $(x_1, 0)$  (see the intersection point of the line  $\beta$  with the

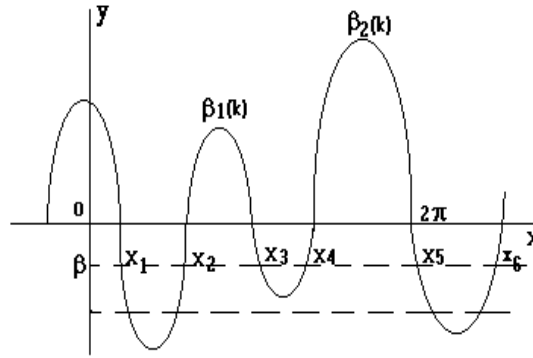


Figure 3

curve  $(\sin x + 2k\sin 2x)$  in Fig.3); if  $\beta = \beta_2$  and  $k > \frac{1}{2}$ , there are three fixed points: one saddle-node  $(x_3, 0)$ , and one center  $(x_1, 0)$  and one saddle  $(x_2, 0)$  (see Fig.3).  $\beta_1$  and  $\beta_2$  are supercritical bifurcation by (2.10).

**Remark.1**  $\beta_1(k)$  and  $\beta_2(k)$  are monotonous function of  $k$ , i.e.,  $\beta_1'(k) > 0, \beta_2'(k) > 0$ , and  $\beta_1 < \beta_2$ , and  $\beta_1(k)$  approaches  $\beta_2(k)$  as  $k$  is large enough. For  $\beta = 0$ , as  $k$  increased the large amplitude heteroclinic orbits in Fig2 contract and the small amplitude heteroclinic orbits in Fig2 expand, up to  $\beta_1(k) \sim \beta_2(k)$ , the amplitude of the two heteroclinic orbits approach.

**Remark.2** We show that for unperturbed system (2.1) there are two qualitatively different periodic solution in the cylinder: (1) the oscillating one (or called as ellipses, or cycle of first type), and the rotating ones (or called as ‘waves’, or cycle of second type); (2) the heteroclinic orbits are the boundaries of the two types of periodic orbits except the saddle-node bifurcation point.

**3. Analysis for perturbed system.** In this section we give the dynamical changes under the perturbations for the Josephson system (A).

**3.1. Damped perturbation.** If the nonlinear damping is added to (2.1), then give the equation

$$\begin{cases} \dot{x} = y \equiv P(x, y), \\ \dot{y} = -\sin x - k\sin 2x + \beta - \epsilon\alpha(\cos x + 2k\cos 2x)y \equiv Q(x, y). \end{cases} \quad (3.1)$$

The phase portraits of unperturbed system (2.1) are destroyed under the perturbation. Besides the existence of fixed points the essential dynamical feature of (3.1) is the presence of four types of two kinds of simple closed orbits and the saddle-to-saddle separatrix loop (heteroclinic orbits) and almost all orbits approach to the fixed point.

The simple closed orbits are cycles of the first kind (those homotopic to zero) corresponding to periodic solutions of (3.1); cycles of the second kind (not homotopic to zero) corresponding to the solution  $y = y(x)$  of the equation  $\frac{dy}{dx} = \frac{Q}{P}$  periodic in  $x$  (and in particular, a constant).

The conditions of the existence for two types of closed orbits and separatrix loop are given by using qualitative method in [16]. We describe the results for system (3.1) as the following, and the detail can be seen in the original literature[16].

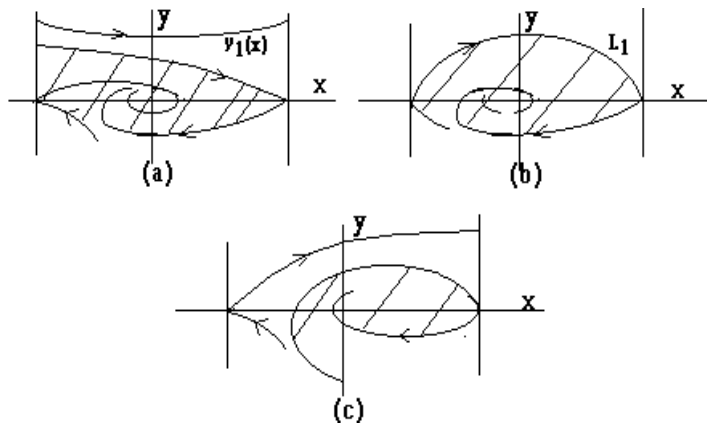


Figure 4. (a)  $\beta = \beta_0^*$ , (b)  $\beta = \beta^*$ , (c)  $\beta > \beta^*$ .

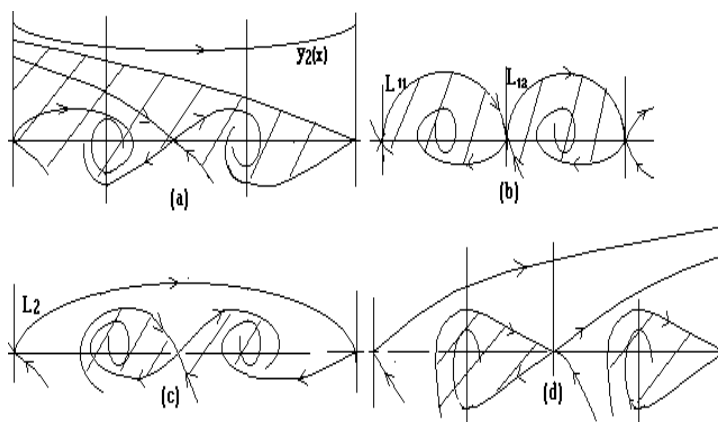


Figure 5. (a)  $\beta = \beta_1^*$ , (b)  $\beta = \beta_{21}^*$ , (c)  $\beta = \beta_{22}^*$ , (d)  $\beta > \beta_{21}^*$  or  $\beta > \beta_{22}^*$ .

**Theorem 3.1** <sup>[16]</sup> For  $0 < k < \frac{1}{2}, 0 < \beta < \beta_1$ , there are two bifurcation values  $\beta_0^*(\alpha, k)$  and  $\beta^*(\alpha, k)$  ( $0 < \beta_0^* < \beta^* < \beta_1$ ) which correspond one unstable cycle  $y_1(x)$  of second type and a separatrix loop  $L_1$  in the half plane  $y > 0$  respectively, and the loop  $L_1$  disappears if  $\beta > \beta^*$  ( $\beta < \beta_1$ ). The global phase portraits changes qualitatively as the parameter  $\beta$  vary which are shown in Fig.4(a)–(c). The cross-hatched areas in Fig.4 show the region of the attraction of the stable equilibrium point.

**Theorem 3.2** <sup>[16]</sup> For  $k > \frac{1}{2}, 0 < \beta < \beta_2$ , there are bifurcation values  $\beta_1^*$  and  $\beta_{21}^*$  or  $\beta_{22}^*$  which correspond one unstable cycle  $y_2(x)$  (see Fig.5(a)) of second type and the represents loop  $L_{11}$  and  $L_{12}$  (see Fig.5(b)) or a separatrix loop  $L_2$  (see Fig.5(c)) in the half plane  $y > 0$  respectively, and the loop  $L_{12}$  and  $L_{22}$  or  $L_2$  disappear if  $\beta > \beta_{21}^*$  or  $\beta > \beta_{22}^*$  (see Fig.5(d)). The cross-hatched areas in Fig.5 show the region of the attraction of the stable equilibrium points.

**Remark 1.** The bifurcation values  $\beta_0^*, \beta^*$ , and  $\beta_1^*, \beta_{21}^*, \beta_{22}^*$  depend on  $\alpha, k$ . But the existence of the  $\beta_{12}^*, \beta_{22}^*$  is not proved up to now, the approximate computation of

the values of the bifurcations in the creation of the separatrix loop and approximate expressions for computation of the catch of the region are given in [16].

**Remark 2.** The system (3.1) is not structurally stable at bifurcation points, since the phase portraits for  $\beta > \beta^*$  and  $\beta < \beta^*$ , or  $\beta > \beta_0^*$  and  $\beta < \beta_0^*$  or  $\beta > \beta_1^*$  and  $\beta < \beta_1^*$  or  $\beta > \beta_2^*$  and  $\beta < \beta_2^*$  are qualitatively different (compare Fig.4(a) and Fig.4(c), Fig.5(a) and Fig.5(d)). Moreover, when  $0 < k < \frac{1}{2}$  for small  $\beta(\beta < \beta^*)$ , both the left and right unstable equilibrium points lie on the boundary of the region of attraction of the stable equilibrium point(see Fig.4(a)), for large  $\beta(\beta > \beta^*)$ , only the right unstable equilibrium point lies on the boundary of the region of attraction of the stable equilibrium point (see Fig.4(c)). When  $k > \frac{1}{2}$ , we also show the different of the boundary of the region of attraction of the stable equilibrium for small  $\beta(\beta < \beta_2^*)$  and large  $\beta(\beta > \beta_2^*)$  (see Fig.5(a) and Fig. 5(d)), where  $\beta_2^* = \beta_{21}^*$  or  $\beta_{22}^*$ .

**3.2. Primary harmonic solutions and bifurcation.** We now study the influence of perturbation (damping and extra force) on the system (2.1), i.e., study the dynamical behavior of Eq.(A). First of all, we consider the primary harmonic solution(primary resonance) of Eq.(A) using the second-order averaging method. Introduce a small parameter  $\epsilon$ , such that  $0 < \epsilon \ll 1$  and replace  $\alpha$  and  $f$  by  $\epsilon\alpha$  and  $\epsilon^{\frac{3}{2}}f$  respectively. Then Eq.(A) can be rewritten as

$$\begin{cases} \dot{x} = y, \\ \dot{y} = -\sin x - k\sin 2x + \beta - \epsilon\alpha(\cos x + 2k\cos 2x)y + \epsilon^{\frac{3}{2}}f \sin \omega t. \end{cases} \quad (3.2)$$

Let  $(x_0, 0)$  be a center of Eq (2.1), i.e.,  $(x_0, 0)$  satisfies

$$-\sin x_0 - k\sin 2x_0 + \beta = 0$$

and

$$\cos x_0 + 2k\cos 2x_0 > 0.$$

The frequency of periodic orbit near the center is approximately given by

$$\omega_0 = \sqrt{\cos x_0 + 2k\cos 2x_0}.$$

If the ratio of  $\omega$  and  $\omega_0$  is a rational number, then resonance behavior may occur in Eq.(3.2). We begin with the case of primary resonance  $\omega \sim \omega_0$  for Eq.(3.2) (hence Eq.(A)). Assume that

$$\begin{aligned} \omega^2 &\sim \omega_0^2, \\ \epsilon\Omega &= \omega^2 - \omega_0^2. \end{aligned}$$

Let

$$a_1 = \cos x_0 + 2k\cos 2x_0 = \omega_0^2, \quad a_2 = -\frac{1}{2}(\sin x_0 + 4k\sin 2x_0), \quad a_3 = \frac{1}{6}(\cos x_0 + 8k\cos 2x_0),$$

and

$$x = x_0 + \sqrt{\epsilon}z, \quad y = y.$$

Then Eq.(3.2) can be rewritten as

$$\ddot{z} + \omega_0^2 z = -a_2\sqrt{\epsilon}z^2 + \epsilon(a_3z^3 - \bar{\alpha}\dot{z} + f\sin\omega t) + O(\epsilon^{\frac{3}{2}}),$$

or

$$\begin{cases} \dot{z} = v_1, \\ \dot{v}_1 = -\omega_0^2 z - a_2\sqrt{\epsilon}z^2 + \epsilon(a_3z^3 - \bar{\alpha}v_1 + f\sin\omega t) + O(\epsilon^{\frac{3}{2}}). \end{cases} \quad (3.3)$$

We use the van der Pol transformation

$$\begin{pmatrix} u \\ v \end{pmatrix} = \begin{pmatrix} \cos\omega t & \frac{1}{\omega}\sin\omega t \\ -\sin\omega t & -\frac{1}{\omega}\cos\omega t \end{pmatrix} \begin{pmatrix} z \\ v_1 \end{pmatrix}$$

and carry out averaging up to second-order for Eq.(3.3). We obtain the following averaged equation:

$$\begin{cases} \dot{u} = \frac{\epsilon}{2\omega_0}(\Omega v - \bar{\alpha}\omega_0 u - b_1(u^2 + v^2)v - f), \\ \dot{v} = \frac{\epsilon}{2\omega_0}(-\Omega u - \bar{\alpha}\omega_0 v + b_1(u^2 + v^2)u). \end{cases} \tag{3.4}$$

where

$$\bar{\alpha} = \alpha\omega_0^2, \quad b_1 = \frac{-(a_1 a_3 \omega_0^2 + 10a_2^2)}{12\omega_0^2} + O(\epsilon).$$

The fixed points of Eq.(3.4) satisfy the following equation:

$$F(u) = b_1^2 f^2 u^3 + 2\Omega b_1 f \bar{\alpha} u^2 + (\bar{\alpha}^2 + \Omega)\bar{\alpha}^2 u + f \bar{\alpha}^3 = 0, \tag{3.5}$$

and

$$v^2 = (-1)u(u + \frac{f}{\bar{\alpha}}). \tag{3.6}$$

In order to find the bifurcation values of the fixed point we write equation (3.5) as

$$F(\bar{u}) = \bar{u}^3 + p\bar{u} + q = 0, \tag{3.7}$$

where

$$\bar{u} = u + \frac{2\Omega b_1 f \bar{\alpha}}{3b_1 f^2}, \quad p = \frac{\bar{\alpha}^2(3\bar{\alpha}^2 - \Omega^2)}{3b_1^2 f^2}, \quad q = \frac{(-18\bar{\alpha}^2\Omega - 2\Omega^3 + 27b_1 f)\bar{\alpha}^3}{27b_1^3 f^3}.$$

At bifurcation points, equation (3.7) must have multiple roots, that is

$$F(\bar{u}) = \bar{u}^3 + p\bar{u} + q = 0, \quad \frac{\partial F}{\partial \bar{u}} = 3\bar{u}^2 + p = 0. \tag{3.8}$$

Now we determine all values of  $p$  and  $q$  (or  $f^2$  and  $\Omega^2$ ) for which equation (3.7) can have some common solution  $\bar{u}$ . If we eliminate  $\bar{u}$  from (3.8), there is the following equation for a cusp:

$$\begin{aligned} \Delta &= 4p^3 + 27q^2 \\ &= 27b_1^2 f^4 - 4(\Omega^2 + 9\bar{u}^2)\Omega b_1 f^2 + 4(\bar{\alpha}^2 + \Omega^2)^2 \bar{\alpha}^2 = 0, \end{aligned} \tag{3.9}$$

The nature of the roots of equation (3.7) (or(3.5)) and hence of the fixed points of the averaged equation (3.4) depends on the position in the  $(\Omega^2, f^2)$ -plane, in relation to the bifurcation curves as

$$\frac{2(\Omega^2 + 9\bar{\alpha}^2) + 2\sqrt{(\Omega^2 - 3\bar{\alpha}^2)^3}}{27b_1} \equiv f_1^2, \tag{3.10}$$

and

$$\frac{2(\Omega^2 + 9\bar{\alpha}^2) - 2\sqrt{(\Omega^2 - 3\bar{\alpha}^2)^3}}{27b_1} \equiv f_2^2, \tag{3.11}$$

In Fig.6 we have drawn the bifurcation curves of Eq.(3.9) in the  $(\Omega^2, f^2)$ -plane. The plane is divided into five subsets in each appropriate region we have sketched a graph for the equation (3.5)(or (3.7)), which include the region (I) “inside” the

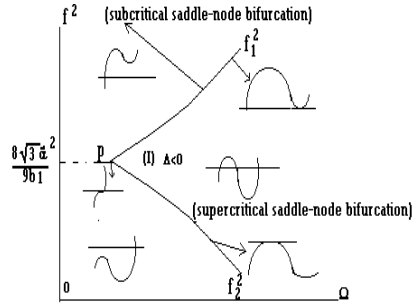


Figure 6

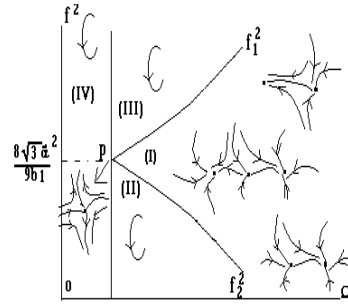


Figure 7

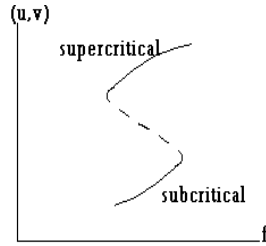


Figure 8

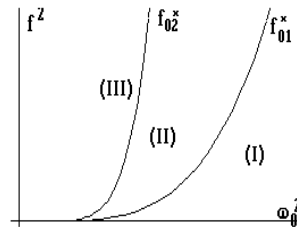


Figure 9

curve  $\Delta = 0$ , the region “outside” it, the two branches  $f_1^2$  and  $f_2^2$  of the curve  $\Delta = 0$ , and the point  $P(p = 0$  and  $q = 0)$ . The points  $(\Omega^2, f^2)$  which lie in (I) are those for  $\Delta < 0$ , those in (E) satisfy  $\Delta > 0$ . Thus, we obtain the following conclusion.

**Lemma 2.** (i) If  $(\Omega^2, f^2)$  lies in (E) there is one real root of Eq.(3.5) which corresponds to one nontrivial fixed point of Eq (3.4).

(ii) If  $(\Omega^2, f^2)$  lies in (I) there are three distinct real roots of (3.5) which correspond to three distinct nontrivial fixed point of Eq.(3.4).

(iii) If  $(\Omega^2, f^2)$  lies in the curve  $f_1^2$  or  $f_2^2$ , there are three real roots of Eq.(3.5), but two of them coincide; on  $f_2^2$  the coincidence occurs for the smaller roots; on  $f_1^2$  the large, which correspond to two nontrivial fixed points of Eq.(3.4).

(iv) If  $(\Omega^2, f^2)$  lies at the point  $P(3\bar{\alpha}^2, \frac{8\sqrt{3}\bar{\alpha}^3}{9b_1})$ , there are three coincident real roots, which correspond to one nontrivial fixed point of Eq.(3.4).

The stability of fixed points  $(u_0, v_0)$  of Eq.(3.4) is determined by the characteristic equation:

$$\lambda^2 + 2\bar{\alpha}\lambda + \bar{\alpha}^2 + \Omega^2 + \frac{3b_1f^2}{\bar{\alpha}^2}u_0^2 + \frac{4b_1\Omega f}{\bar{\alpha}}u_0 = 0, \tag{3.12}$$

Thus, the fixed point  $(u_0, v_0)$  is stable if the following condition holds:

$$g(u_0) = b_1^2f^2u_0^3 + 2\Omega b_1f\bar{\alpha}u_0^2 + (\bar{\alpha}^2 + \Omega^2)\bar{\alpha}^2u_0 + f\bar{\alpha}^3 > 0, \tag{3.13}$$

and the fixed point  $(u_0, v_0)$  is a stable node if  $0 < g(u_0) < \bar{\alpha}^2$ ; is a stable focus if  $g(u_0) > \bar{\alpha}^2$ . It is obvious that the fixed point  $(u_0, v_0)$  is unstable if  $g(u_0) < 0$ ,

meanwhile we can prove that  $\frac{\partial^2 F}{\partial u^2} \frac{\partial F}{\partial f} |_{f_1^2} > 0$  and  $\frac{\partial^2 F}{\partial u^2} \frac{\partial F}{\partial f} |_{f_2^2} < 0$ .

Moreover, by the Dulac’s criterion it is known that the averaged equation (3.4) has no closed orbit.

Thus, by consider the above stability conditions and the roots of Eq.(3.5) we can obtain the phase portraits which are given in Fig.7 and the following conclusion:

**Lemma 3.** (i) For  $\Omega^2 - 3\bar{\alpha}^2 > 0$  and  $0 < \epsilon \ll 1$ , there exist two stable foci-node and one saddle in region (I); there exists a stable foci-node in region (II) and (III). From region (I) to (II) or to (III), the supercritical saddle-node bifurcation of fixed point occurs at the curve  $f_2^2$ , the subcritical saddle-node bifurcation occurs at the curve  $f_1^2$ . On the curves  $f_1^2$  and  $f_2^2$  there are one stable foci-node and one saddle-node.

(ii) For  $\Omega^2 - 3\bar{\alpha}^2 < 0$  and  $0 < \epsilon \ll 1$ , there exists a stable foci-node in the region (IV);

(iii) For  $\Omega^2 - 3\bar{\alpha}^2 = 0$  and  $0 < \epsilon \ll 1$ , there exists a stable foci-node on the line  $\Omega^2 = 3\bar{\alpha}^2$ ;

(iv) At the point P, there exists a saddle;

(v) When  $f_2^2$  is increasing, the fixed point is changed from one into three, through passing  $f_2^2$ , on the  $f_2^2$  there are two fixed points and one of them is saddle-node, so the  $f_2^2$  is supercritical saddle-node bifurcation; when  $f_1^2$  is decreasing, the fixed point is changed from one to three, on  $f_1^2$  there are two fixed points and one of them is saddle-node, so the  $f_1^2$  is subcritical saddle-node bifurcation. Fig.8 shows a bifurcation diagram indicating how the fixed point of Eq.(3.4) are created or annihilated when  $f$  is varying while the other parameters remain fixed.

By the averaging theorem (see [24]), the hyperbolic fixed points of the averaged equation (3.4) correspond to the resonant harmonic solutions of the original equation (3.2) and therefore asymptotically to solutions of Eq.(A) for sufficiently small value of  $\epsilon \neq 0$ . For all other solutions of (3.4) the asymptotic validity is for a finite interval of time proportional to  $\epsilon^{-1}$ .

Therefore, by Lemma1-2 and the averaging theorem for Eq.(3.2) (or Eq.(A)) we can give the following Theorem.

**Theorem 3.3** (i) For  $\Omega^2 - 3\bar{\alpha}^2 > 0$  and  $0 < \epsilon \ll 1$ , there exists two stable resonant harmonic solutions and one unstable resonant harmonic solution in region (I), there is a stable resonant harmonic in region (II) and (III). A stable harmonic appears near the supercritical bifurcation curve  $f_2^2$  and a stable harmonic disappears near the subcritical bifurcation curve  $f_1^2$ .

(ii) For  $\Omega^2 - 3\bar{\alpha}^2 \leq 0$  and  $0 < \epsilon \ll 1$ , there exists a stable harmonic in region (IV) and on the line  $\Omega^2 = 3\bar{\alpha}^2$ .

(iii) At the point  $P(3\bar{\alpha}^2, \frac{8\sqrt{3\bar{\alpha}^2}}{9b_1})$ , there exists an unstable harmonic solution.

(iv) The harmonic solutions of Eq.(3.2) is approximately given by

$$x(t) = x_0(t) + \sqrt{\epsilon}(u\cos\omega t - v\sin\omega t) + O(\epsilon)$$

where  $u$  and  $v$  are given by the equilibrium solutions of averaged equation (3.4). The other solutions in Eq.(3.4) correspond to the almost periodic solutions or chaotic motions in Eq.(3.2) (or Eq.(A)).

Where  $f_1^2$  and  $f_2^2$  are given in (3.10) and (3.11) respectively, and  $\bar{\alpha} = \alpha\omega_0^3$ .

**3.3. Subharmonic solutions and bifurcations.** In this subsection we investigate the second-order subharmonic resonance (secondary resonance) and  $n$ -order subharmonics using the second-order averaging method and the Melnikov method

respectively. For second order subharmonic resonance  $\omega \approx 2\omega_0$ , we set

$$\epsilon\Omega = \frac{\omega^2 - 4\omega_0^2}{4}.$$

Replacing  $\alpha$  and  $f$  by  $\epsilon\alpha$  and  $\epsilon f$  ( $0 < \epsilon \ll 1$ ) respectively, then Eq.(A) can be written as

$$\begin{cases} \dot{x} = y, \\ \dot{y} = -\sin x - k\sin 2x + \beta - \epsilon\alpha(\cos x + 2k\cos 2x)y + \epsilon f \sin \omega t. \end{cases} \quad (3.14)$$

Using regular perturbation methods, one obtains harmonics of (3.14) in the form  $x(t) = x_0 - \epsilon\Gamma \sin \omega t + O(\epsilon^2)$ , where  $\Gamma = \frac{f}{\omega^2 - \omega_0^2}$ . (Assume  $x(t, \epsilon) = x_0 + \epsilon x_1 + \dots$  substituted into (3.14), we obtain

$$x_0 = a_0 \cos \omega t + b_0 \sin \omega t$$

and

$$x_1 = -\frac{f}{\omega^2 - \omega_0^2} \sin \omega t,$$

hence

$$x(t) = x_0 + \epsilon x_1 = x_0 - \epsilon\Gamma \sin \omega t.$$

To investigate stability of the harmonic  $x(t)$ , one can set

$$x = x_0 + \sqrt{\epsilon}z - \epsilon\Gamma \sin \omega t, \quad (3.15)$$

where  $(x_0, 0)$  is a center of Eq.(3.14) for  $\epsilon = 0$ .

Substituting (3.15) into (3.14), then Eq.(3.14) becomes as

$$\ddot{z} = -a_1 z - \sqrt{\epsilon}a_2 z^2 + \epsilon(a_3 z^3 - \alpha a_1 \dot{z} + 2a_2 \Gamma z \sin \omega t) + O(\epsilon^{\frac{3}{2}}). \quad (3.16)$$

We use the van der Pol transformation

$$\begin{pmatrix} u \\ v \end{pmatrix} = \begin{pmatrix} \cos \frac{\omega t}{2} & -\frac{2}{\omega} \sin \frac{\omega t}{2} \\ -\sin \frac{\omega t}{2} & -\frac{2}{\omega} \cos \frac{\omega t}{2} \end{pmatrix} \begin{pmatrix} z \\ \dot{z} \end{pmatrix} \quad (3.17)$$

and carry out averaging up to second-order, so that the averaged equation corresponding Eq.(3.16) becomes as

$$\begin{cases} \dot{u} = \frac{\epsilon}{2\omega_0} [\Omega v - (\alpha a_1 \omega_0 + \frac{a_2 \Gamma}{4})u + c(u^2 + v^2)v] \equiv P(x, y), \\ \dot{v} = \frac{\epsilon}{2\omega_0} [-\Omega u - (\alpha a_1 \omega_0 - \frac{a_2 \Gamma}{4})v - c(u^2 + v^2)u] \equiv Q(x, y), \end{cases} \quad (3.18)$$

where

$$c = \frac{3a_3}{4} + \frac{10a_2^2}{24\omega_0^2}.$$

By the Dulac's criterion we know that

$$\frac{\partial P}{\partial u} + \frac{\partial Q}{\partial v} = -2\alpha a_1 \omega_0. \quad (3.19)$$

and no periodic solution for Eq.(3.18).

For Eq.(3.18) apart from the trivial fixed point  $(0, 0)$ , the nontrivial fixed points satisfy the following equations

$$\frac{c^2 a_2^2 \Gamma^2}{4(\alpha a_1 \omega_0 + \frac{a_2 \Gamma}{4})^2} v^4 + \frac{\Omega a_2 c \Gamma}{\alpha a_1 \omega_0 + \frac{a_2 \Gamma}{4}} v^2 + (\Omega^2 + \alpha^2 a_1^2 \omega_0^2 - \frac{a_2^2 \Gamma^2}{16}) = 0, \quad (3.20)$$

There therefore exist nontrivial fixed points for Eq.(3.18) if the following conditions are satisfied:

$$f_{02}^* \equiv \frac{144\omega_0^2(\Omega^2 + \alpha^2 a_1^2 \omega_0^2)}{a_2^2} > f^2 \geq \frac{144\alpha^2 a_1^2 \omega_0^4}{a_2^2} \equiv f_{01}^*,$$

and  $c > 0$ .

The eigenvalue equation about the fixed point  $(0, 0)$  in Eq.(3.18) satisfy the following equation

$$\lambda^2 + 2\alpha a_1 \omega_0 \lambda + 4(\Omega^2 + \alpha^2 a_1^2 \omega_0^2) - \frac{a_2^2 f^2}{36\omega_0^4}, \quad (3.21)$$

Let

$$D(\omega_0) = 4(\Omega^2 + \alpha^2 a_1^2 \omega_0^2) - \frac{a_2^2 f^2}{36\omega_0^4}$$

For the stability and bifurcation of the fixed point  $(0, 0)$  of Eq.(3.18) we have the following conclusion:

**Lemma 4.** *There exists a bifurcation  $l$  which is given by*

$$f^2(\omega_0) = \frac{144\omega_0^2(\Omega^2 + \alpha^2 a_1^2 \omega_0^2)}{a_2^2} \equiv f_{02}^*. \quad (3.22)$$

Moreover, above the  $l$  the fixed point  $(0, 0)$  is stable, below the  $l$  the fixed point  $(0, 0)$  is unstable; on the bifurcation curve  $l$  the fixed point is a saddle-node (one eigenvalue  $\lambda_1 = 0$  and another  $\lambda_2 = -2\alpha a_1 \omega_0$ ).

The eigenvalue equations about the nontrivial fixed point  $(u_0, v_0)$  of Eq.(3.18) satisfy the following equations:

$$\begin{aligned} \lambda^2 + 2\alpha a_1 \omega_0 \lambda - (2cu_0 v_0 - (\alpha a_1 \omega_0 + \frac{a_2 \Gamma}{4}))(2cu_0 v_0 + (\alpha a_1 \omega_0 - \frac{a_2 \Gamma}{4})) \\ + (\Omega + 3cv_0^2 + cu_0^2)(\Omega + 3cv_0^2 + cv_0^2) = 0. \end{aligned}$$

Let

$$\begin{aligned} G(u_0, v_0) = -(2cu_0 v_0 - (\alpha a_1 \omega_0 + \frac{a_2 \Gamma}{4}))(2cu_0 v_0 + (\alpha a_1 \omega_0 - \frac{a_2 \Gamma}{4})) \\ + (\Omega + 3cv_0^2 + cu_0^2)(\Omega + 3cv_0^2 + cv_0^2). \end{aligned} \quad (3.23)$$

Therefore, the fixed point  $(u_0, v_0)$  is a stable if  $G(u_0, v_0) > 0$ , and a unstable if  $G(u_0, v_0) < 0$ .

By the averaging theorem and the above analysis we get the following conclusion:

**Theorem 3.4.** *(i) Including the trivial fixed point  $(0, 0)$ , there are one, three, or five fixed points in Eq. (3.18). Each additional pair of nontrivial fixed points corresponds to a single subharmonic of period two of Eq. (3.14) and is given approximately by*

$$x(t) = x_0 + \sqrt{\epsilon}(u_0 \cos \frac{\omega t}{2} - v_0 \sin \frac{\omega t}{2}) - \epsilon \Gamma \sin \omega t,$$

where  $(u_0, v_0)$  is the solution of Eq. (3.18).

*The trivial fixed point  $(0, 0)$  corresponds to a non-resonance harmonic of Eq. (3.14).*

*(ii) There are two bifurcation curves which are given by*

$$f^2 = \frac{144\alpha^2 a_1^2 \omega_0^4}{a_2^2} \equiv f_{01}^*, \tag{3.24}$$

and

$$f^2 = \frac{144\omega_0^2(\Omega^2 + \alpha^2 a_1^2 \omega_0^4)}{a_2^2} \equiv f_{02}^*. \tag{3.25}$$

$f_{02}^*$  is the supercritical bifurcation or the period-doubling bifurcation of harmonic, and  $f_{01}^*$  is the subcritical bifurcation or the saddle-node bifurcation of subharmonic. The curves  $f_{01}^*$  and  $f_{02}^*$  are given by the numerical simulation in Fig.9.

(iii) See Fig.9: in region (I) there is a stable fixed point (0,0) of Eq.(3.18), which corresponds to a stable non-resonant harmonic of Eq.(3.14); on the curve  $f_{01}^*$  there are three fixed points which correspond to a stable non-resonant harmonic and a single unstable resonant subharmonic of period-two of Eq.(3.14). In region(II) there are five fixed points which correspond to a stable harmonic and two resonant subharmonic (one stable and another unstable) of period-two of Eq.(3.14). On the curve  $f_{02}^*$  there are three fixed points which correspond to a saddle-node harmonic and a unstable subharmonic. In region (III) the harmonic becomes unstable and the unstable subharmonic disappears.

From above analysis we show that there exist second-order subharmonic solutions for  $f_{01}^* < f^2 < f_{02}^*$ , and there exist only harmonic solution for  $f^2 < f_{01}^*$  and  $f^2 > f_{02}^*$ . We give the harmonic solution and subharmonic solution in phase-plane by the numerically simulations for fixed parameters  $k = 0.8, \alpha = \beta = 0.001$  and varying  $f$  and  $\omega$ .

There are harmonic solutions for  $f = 0$  and  $\omega = 0$ (Fig.10), and  $f = 60, \omega = 1$  (Fig.11), but the amplitude for  $f = 60$  is thirty fold of  $f = 0$ , and there are subharmonic solutions for  $f = 0.1$  and  $\omega = 1$  (see Fig.12).

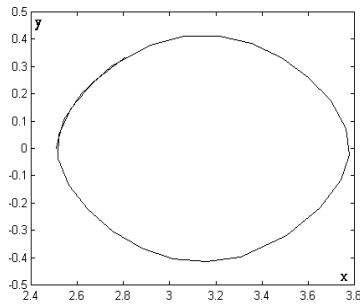


Figure 10

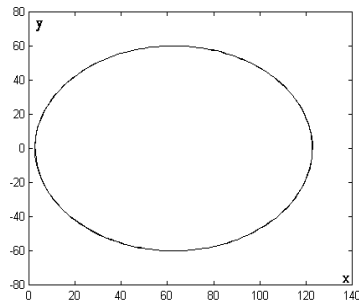


Figure 11

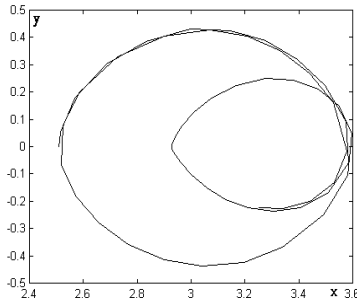


Figure 12

In order to investigate the existence of  $n$ -order subharmonic solutions of Eq.(3.14), we use the Melnikov function for subharmonic which is defined as [13, 31].

In the following we shall consider two different type of the perturbed system

$$\begin{cases} \dot{x} = y, \\ \dot{y} = -\sin x - k\sin 2x + \beta - \epsilon[\alpha(\cos x + 2k\cos 2x)y - f\sin\omega t]. \end{cases} \quad (3.26)$$

$$\begin{cases} \dot{x} = y, \\ \dot{y} = -\sin x - k\sin 2x - \epsilon[\alpha(\cos x + 2k\cos 2x)y - \beta - f\sin\omega t]. \end{cases} \quad (3.27)$$

When  $\epsilon = 0$  write (3.26) and (3.27) as  $(3.26)_0$  and  $(3.27)_0$  respectively.

Consider a one-parameter family of periodic orbits  $q^\mu(t) = (x^\mu, y^\mu)$  with  $\mu$  in  $(\mu_1, \mu_2)$ , where  $\mu_1$  and  $\mu_2$  are constants, let  $q^\mu(t)$  and  $q_1^\mu(t)$  be a periodic orbit of period  $\frac{2\pi m}{\omega}$  of Eq (3.26)<sub>0</sub> and (3.27)<sub>0</sub> respectively, where  $m$  is a positive integer. In [33] it has been proved that  $M^{\frac{m}{n}}(t_0)$  can have simple zero only if  $n = 1$ , so the Melnikov function for  $q^\mu(t)$  of Eq.(3.26) is given by

$$\begin{aligned} M^m(t_0) &= \int_0^{\frac{2\pi m}{\omega}} y^\mu(t)[- \alpha(\cos(x^\mu(t)) + 2k\cos(2x^\mu(t)))y^\mu(t) + f\sin\omega(t + t_0)]dt \\ &= \int_0^{\frac{2\pi m}{\omega}} -\alpha(\cos x^\mu(t) + 2k\cos(2x^\mu(t)))(y^\mu(t))^2 dt + f \int_0^{\frac{2\pi m}{\omega}} y^\mu(t)\sin\omega t\cos\omega t_0 dt \\ &\quad + f \int_0^{\frac{2\pi m}{\omega}} y^\mu(t)\sin\omega t_0\cos\omega t dt = -\alpha A^m(\beta, k, \omega) + f\cos\omega t_0 B^m(\beta, k, \omega) + \\ &\quad f\sin\omega t_0 C^m(\beta, k, \omega) = -\alpha A^m + fS^m \sin(\omega t_0 + \Theta^m(\omega)), \end{aligned} \quad (3.28)$$

where

$$\begin{aligned} A^m(\beta, k, \omega) &= \int_0^{\frac{2\pi m}{\omega}} (y^\mu(t))^2 (\cos(x^\mu(t)) + 2k\cos(2x^\mu(t))) dt, \\ B^m(\beta, k, \omega) &= \int_0^{\frac{2\pi m}{\omega}} y^\mu(t)\sin\omega t dt, \\ C^m(\beta, k, \omega) &= \int_0^{\frac{2\pi m}{\omega}} y^\mu(t)\cos\omega t dt \\ S^m(\beta, k, \omega) &= \sqrt{(B^m)^2 + (C^m)^2}, \\ \Theta^m(\omega) &= \arctan \frac{B^m}{C^m}. \end{aligned} \quad (3.29)$$

If

$$\frac{f}{\alpha} \geq \frac{A^m}{S^m} \equiv R_1^m(\beta, k, \omega), \quad (3.30)$$

then  $M^m(t_0)$  has simple zero and a necessary condition for the occurrence of subharmonics of period  $\frac{2\pi m}{\omega}$  of Eq.(3.26) is given by (3.30).

The bifurcation curve of subharmonics is created and occurs at

$$\frac{f}{\alpha} \equiv R_1^m(\beta, k, \omega) + O(\epsilon). \quad (3.31)$$

The bifurcation curve (3. 31) is shown for  $k = 0.8, \epsilon = 0.01, \beta = 0.001, \alpha = 3, f = 2, \omega = 3$  in Fig.13 in the  $(\omega, \frac{f}{\alpha})$  parameter plane, which separate regions with and without occurrence of subharmonics.

The Melnikov function for  $q_1^\mu(t)$  of Eq.(3.27) is given by

$$M_1^m(t_0) = \int_0^{\frac{2\pi m}{\omega}} y_1^\mu(t)[- \alpha\cos(x_1^\mu(t))$$

$$\begin{aligned}
& +2k\cos(2x_1^\mu(t))y_1^\mu(t) + \beta + f\sin\omega(t+t_0)]dt \\
= & -\alpha \int_0^{\frac{2\pi m}{\omega}} (\cos x_1^\mu(t) + 2k\cos(2x_1^\mu(t)))(y_1^\mu(t))^2 dt + \beta \int_0^{\frac{2\pi m}{\omega}} y_1^\mu(t) dt \\
& + f \int_0^{\frac{2\pi m}{\omega}} y_1^\mu(t) \sin\omega t \cos\omega t_0 dt + f \int_0^{\frac{2\pi m}{\omega}} y_1^\mu(t) \sin\omega t_0 \cos\omega t dt \\
= & -2\alpha \int_{x_1^0}^{x_2^0} (y_1^\mu(t))^2 (\cos x_1^\mu(t) + 2k(\cos 2x_1^\mu(t))) dt \\
+ 2\beta & (x(\frac{T^m}{2}) - x(0)) + 2f \int_{x_1^0}^{x_2^0} \sin\omega t \cos\omega t_0 dx + 2f \int_{x_1^0}^{x_2^0} \sin\omega t_0 \cos\omega t dx \\
= & -2\alpha A_1^m(k, \omega) + 2\beta B_1 + 2f C_1^m(k, \omega) \cos\omega t_0 + 2f D_1^m(k, \omega) \sin\omega t_0 \\
= & -2\alpha A_1^m + 2\beta B_1 + 2S_1^m \sin(\omega t_0 + \Theta_1^m(\omega)). \tag{3.32}
\end{aligned}$$

where  $x_1^0$  and  $x_2^0$  are the two points at which the periodic orbit  $q_1^\mu(t)$  crosses the  $x$ -axis in the phase-plane and

$$\begin{aligned}
A_1^m &= \int_{x_1^0}^{x_2^0} y^2(\cos(x + 2k\cos 2x)) dx, \\
B_1 &= x(\frac{T^m}{2}) - x(0), \\
C_1^m &= \int_{x_1^0}^{x_2^0} \sin\omega \left( \int_{x_1^0}^{x_2^0} \frac{dx}{\sqrt{2H^m + 2\cos x + k\cos 2x}} \right) dx, \\
D_1^m &= \int_{x_1^0}^{x_2^0} \cos\omega \left( \int_{x_1^0}^{x_2^0} \frac{dx}{\sqrt{2H^m + 2\cos x + k\cos 2x}} \right) dx, \\
S_1^m &= \sqrt{(C_1^m)^2 + (D_1^m)^2}, \\
\Theta_1^m &= \arctan \frac{C_1^m}{D_1^m}.
\end{aligned}$$

It follows that for fixed  $k$  and  $\omega$  if

$$f \geq \left| \frac{\alpha A_1^m - \beta B_1}{S_1^m} \right| \equiv R_2^m(k, \omega, \alpha, \beta). \tag{3.33}$$

Then  $M_1^m(t_0)$  has simple zero and the bifurcation curve of  $m$ -order subharmonics is created and occurs at

$$f = R_2^m(k, \omega, \alpha, \beta). \tag{3.34}$$

The bifurcation curve (3.34) for  $k = 0.8$ ,  $\alpha = 3$ ,  $\epsilon = 0.01$ ,  $\beta = 0.001$  is shown in Fig.14 in the  $(\omega, \frac{f}{\alpha})$  parameter plane which separate regions with and without occurrence of subharmonics. By the above analysis for subharmonics Melnikov function we find that the bifurcation formulae (3.30) of Eq.(3.26) (corresponds to the bifurcation curve in Fig.13) differ from the bifurcation formula (3.33) of Eq.(3.27) (corresponds to the bifurcation curve in Fig.14). The bifurcation curve Fig.14 may

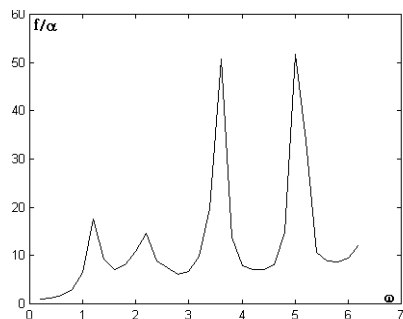


Figure 13

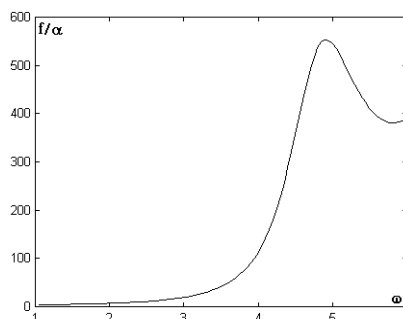


Figure 14

be considered a more smooth, and the bifurcation curve Fig.13 present the oscillations, since the different of the perturbed terms between (3.26) and (3.27).

**4. Heteroclinic bifurcation for chaos.** In this section, we write Eq.(A) as the following three different perturbed forms:

$$\begin{cases} \dot{x} = y \equiv f_1(x, y) + \epsilon g_1(x, y, t), \\ \dot{y} = -\sin x - k\sin 2x - \epsilon[\alpha(\cos x + 2k\cos 2x)y - \beta - f\sin\omega t], \\ \equiv f_2(x, y) + \epsilon g_2(x, y, t). \end{cases} \quad (4.1)$$

$$\begin{cases} \dot{x} = y \equiv f_1(x, y) + \epsilon g_1(x, y, t), \\ \dot{y} = -\sin x - k\sin 2x + \beta - \epsilon[\alpha(\cos x + 2k\cos 2x)y - f\sin\omega t], \\ \equiv f_2(x, y) + \epsilon g_2(x, y, t). \end{cases} \quad (4.2)$$

$$\begin{cases} \dot{x} = y \equiv f_1(x, y) + \epsilon g_1(x, y, t), \\ \dot{y} = -\sin x - k\sin 2x - \alpha(\cos x + 2k\cos 2x)y + \beta + \epsilon f\sin\omega t \\ \equiv f_2(x, y) + \epsilon g_2(x, y, t). \end{cases} \quad (4.3)$$

where  $0 \leq \epsilon \ll 1$  and  $\alpha, \beta, f$ , are of order one for (4.1), and  $\alpha, f$  are of order one for (4.2), and  $f$  is of order one for (4.3). Let  $\epsilon = 0$ , Eqs.(4.1)-(4.3) become three different unperturbed systems  $(4.1)_0$ -(4.3)<sub>0</sub>, respectively. Moreover,  $(4.1)_0$  and  $(4.2)_0$  are Hamiltonian, and possess heteroclinic orbits as Fig.2. Eq.(4.3)<sub>0</sub> is non-Hamiltonian system, but we have proved the existence of heteroclinic orbit in the half-cylinder  $y \geq 0$  for  $\beta = \beta^*(\alpha, k)$  as Fig.5(b) or Fig.5(c) by qualitative method and numerically simulation in [16]. When the perturbations are added ( $\epsilon \neq 0$ ), Eqs.(4.1)-(4.3) may have transverse heteroclinic orbits. By the Smale-Birkhoff Theorem [13,30, 31], the existence of such orbits results in chaotic dynamics. And we can apply Melnikov's method to Eqs.(4.1)-(4.3) and obtain criteria for the existence of heteroclinic bifurcation and chaos.

The conditions of the Melnikov function  $M(t_0)$  has transverse zeros for Eqs(4.1) and (4.3) are given in [17]. Moreover, we give the expression for the Melnikov function and the changes of regions of chaos as  $k$  increases (see Fig.15) for Eq.(4.1). The curves  $C_i(i = 1 - 4)$  in Fig.15 correspond to the Melnikov integrals for different

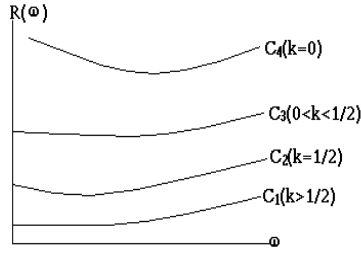


Figure 15

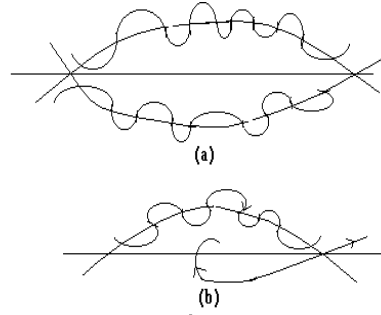


Figure 16

$k$ , and separated the regions with and without occurrence of chaos. Above the curves  $C_i (i = 1 - 4)$  the “double chaotic” arise in Eq.(4.1) (as in Fig.16(a)). The “double chaotic” means both branches of the stable and unstable manifolds intersect transversely in the cylinder.

For the non-Hamiltonian system (4.3), we have proved the existence of heteroclinic orbits for  $\beta = \beta^*(\alpha, k)$  and chaotic dynamics in the half-cylinder  $y \geq 0$  (as in Fig.16(b)) in Eq.(4.3) by qualitative analysis and Melnikov method.

We now give the heteroclinic bifurcation criteria of chaos in Eq.(4.2).

The unperturbed system ( $\epsilon = 0$ ) for Eq.(4.2) is Hamiltonian system with energy given by Eq.(2.2) and has the two types of heteroclinic orbits

$$\Gamma_{13}^{\pm}(t)(x_{13}^{\pm}(t), y_{13}^{\pm}(t))$$

and

$$\Gamma_{35}^{\pm}(t)(x_{35}^{\pm}(t), y_{35}^{\pm}(t))$$

associated with hyperbolic saddle points  $(x_1, 0)$ ,  $(x_3, 0)$  and  $(x_5, 0)$  for  $0 \leq x \leq 2\pi$  (see Fig.1). The Melnikov function for Eq.(4.2) is

$$\begin{aligned} M^m(t_0) &= \int_{-\infty}^{\infty} y(t)[- \alpha y(t)(\cos x(t) + 2k\cos(2x(t))) + f\sin\omega(t + t_0)]dt \\ &= -\alpha l_1(k, \beta, \omega) - 2k\alpha l_2(k, \beta, \omega) + fl_3(k, \beta, \omega)\cos\omega t_0 + fl_4(k, \beta, \omega)\sin\omega t_0 \\ &= -\alpha l_1 - 2k\alpha l_2 + fA\sin(\omega t_0 + \theta). \end{aligned} \tag{4.4}$$

where

$$\begin{aligned} l_1(k, \beta, \omega) &= \int_{-\infty}^{\infty} (y(t))^2 \cos x(t) dt, & l_2(k, \beta, \omega) &= \int_{-\infty}^{\infty} (y(t))^2 \cos 2x(t) dt, \\ l_3(k, \beta, \omega) &= \int_{-\infty}^{\infty} y(t) \sin \omega t dt, & l_4(k, \beta, \omega) &= \int_{-\infty}^{\infty} y(t) \cos \omega t dt, \\ A(k, \beta, \omega) &= \sqrt{l_3^2 + l_4^2}, & \theta &= \arctan \frac{l_3}{l_4}. \end{aligned} \tag{4.5}$$

Note that  $(x(t), y(t))$  in (4.4) is given by

$$(x_{13}(t), y_{13}(t)), (x_{31}(t), y_{31}(t))$$

and

$$(x_{35}(t), y_{35}(t)), (x_{53}(t), y_{53}(t))$$

for the heteroclinic orbits  $\Gamma_{13}(t)$ ,  $\Gamma_{31}(t)$  and  $\Gamma_{35}(t)$ ,  $\Gamma_{53}(t)$ , respectively.

Let  $M(t_0) = 0$ , we have

$$M(t_0) = -\alpha l_1 - 2k\alpha l_2 + fA\sin(\omega t_0 + \theta) = 0.$$

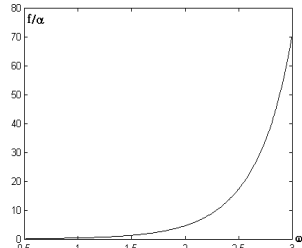


Figure 17

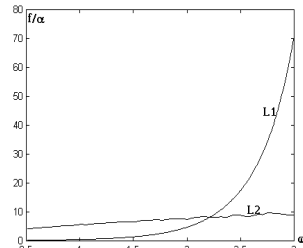


Figure 18

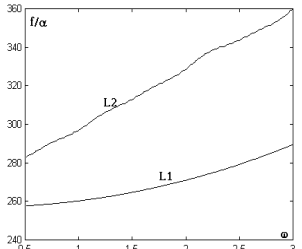


Figure 19

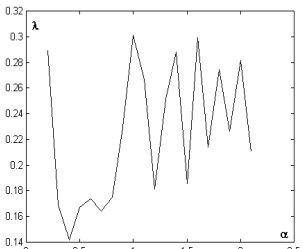


Figure 20

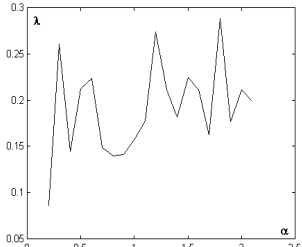


Figure 21

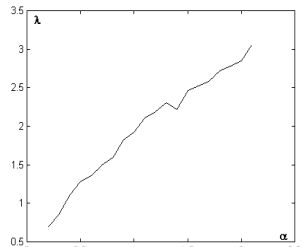


Figure 22

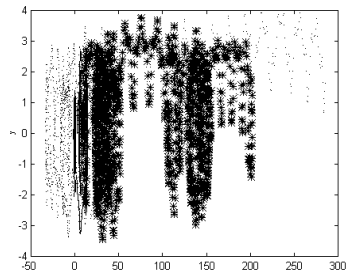


Figure 23

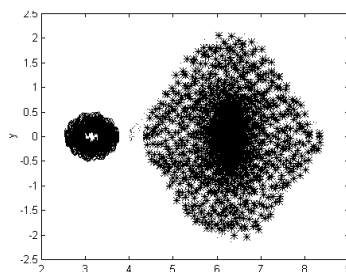


Figure 24

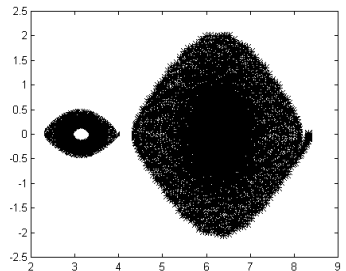


Figure 25

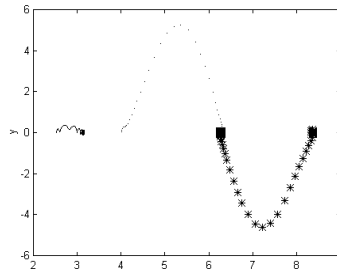


Figure 26

Thus, if

$$\frac{f}{\alpha} > \left| \frac{l_1 + 2kl_2}{4} \right| \equiv R(\omega), \tag{4.6}$$

then there is a  $t_0$  such that  $M(t_0) = 0$  and  $\frac{dM}{dt}|_{t_0} \neq 0$ , and obtain the following conclusion:

**Theorem 4.** *The heteroclinic bifurcation of Eq.(4.2) will occur if*

$$\frac{f}{\alpha} = R(\omega). \quad (4.7)$$

This implies that Eq.(4.7) represents a criteria for the existence of Smale-horseshoe chaos in Eq.(4.2).

The bifurcation curves in the  $(\omega, \frac{f}{\alpha})$  parameter plane which separates regions with and without occurrence of chaos is given by equality in formula (4.6). The heteroclinic bifurcation curves by the numerical simulation for (4.7) and fixed  $\beta = 0.0001$  are shown in Fig.17–19 for  $k = 0.2, k = 0.8$ , and  $k = 30.5$ , respectively. Fig.18 and Fig.19 depict heteroclinic bifurcation curves  $l_1$  and  $l_2$  which are corresponding the bifurcations of the heteroclinic orbits from  $(x_1, 0)$  to  $(x_3, 0)$ , and from  $(x_3, 0)$  to  $(x_5, 0)$ , respectively. We note that the heteroclinic bifurcation curves for fixed  $\beta = 0.0001$  and different values  $k$ , for example,  $k = 0.2$ (Fig.17),  $k = 0.8$ (Fig.18) and  $k = 30.5$  (Fig.19), and for the two types of heteroclinic orbits in same value  $k$  (compare the two curves  $l_1$  (is for the bifurcation from  $(x_1, 0)$  to  $(x_3, 0)$ ) and  $l_2$  (is for the bifurcation from  $(x_3, 0)$  to  $(x_5, 0)$ ) in Fig.18 and Fig.19) are different.

The chaotic behavior in Eq.(A) is also verified by Lyapunov exponent. For Eq.(4.2), we calculated the Lyapunov exponent as a function of parameter  $\alpha$  as show in Fig.20–22 corresponding cases:  $k = 0.2, k = 0.8$  and  $k = 30.5$  and fixed  $\beta = 0.0001, \varepsilon = 0.01, f = 2, \omega = 3$ , respectively. We shown that the Lyapunov exponent is positive and the motion is chaotic when  $\alpha \geq 0.2$  for above cases.

Here we report some of chaotic behaviors by numerical investigate. One interesting result is that the driving frequency  $\omega$  effects to the form of attractor of the trajectory. For example, for fixed  $k = 0.8, \beta = 0.001, \alpha = 0.01$  and  $f = 0.8$ , vary  $\omega$ :

(i). If  $\omega = 0.8$ , there are the chaotic trajectories with a cloud nonregular points at the regions of the initial points  $(2.521, 0)$ ,  $(4.032, 0)$  and  $(8.33, 0)$  which are the approximate saddle points of the unperturbed system  $(4.1)_0$  ( see Fig.23).

(ii). If  $\omega = 6.8$ , we show that the chaotic trajectories with the obvious boundaries(see Fig.24), and the left of that is from initial  $(2.521, 0)$ , and the right of that is from initials  $(4.032, 0)$  and  $(8.33, 0)$ . And moreover, for  $0.2 \leq f \leq 2$  and  $6.5 \leq \omega \leq 25$  there are analogous chaotic trajectories. In particular, if  $\omega = 25$ , the  $n(> 20)$ -subharmonic trajectories are include in the chaotic motions(see Fig.25).

If fixed  $k = 0.8, \beta = 0.001, \alpha = 3, f = 0.8$  and  $\omega = 6.8$ , the trajectories with initials  $(2.521, 0)$ ,  $(4.032, 0)$  and  $(8.33, 0)$  are tending the three different attractors with the very small size, respectively ( see Fig.26).

**5. Conclusion.** The study of the Josephson System.(A) has revealed a rich content of dynamical behavior, which including limit cycles, harmonic and subharmonic bifurcations, and chaotic motions as the parameters vary. Combining our previous results from the literature [16, 17] with our new results we proved more complete descriptions of the Josephson System (A). However, Josephson System (A) still have not been completely discussed, because the parameter space is so large. There are at least the following problems should consider in the future studies.

(1). Chaos is not difficult to find by numerical simulations, however, the analytic investigation may be difficult, for examples, give the analytic conditions of

various routes to chaos (period-doubling bifurcation, period-three-triple bifurcation, intermittence chaos).

(2). Future numerical simulations should attempt to study: find out an various attractors and effect of parameters and initial condition on the dynamic.

**Acknowledgements.** The authors wish to thank Dr. Pengcheng Xu for his help in the numerical simulations.

## REFERENCES

- [1] Belyky, V.N., Pedersen, N.F. and Soerensen, O.H., *Shunted-Josephson model, I. The autonomous, II. The non-autonomous case*, Phys. Rev. B., 16 (1977), 4853–4871.
- [2] Ben-Jacobi, E., Goldhirsch, I., Imry, Y. and Fishman, S., *Intermittent chaos in Josephson junctions*, Phys. Rev. Lett., 49 (1982), 1599–1602.
- [3] Chua, L.O. and Tang, Y.S., *Nonlinear oscillation via voltage series*, IEEE Trans, Circuits Syst., AS-2913 (1982), 150–168.
- [4] Chua, L.O., Desoe, C.A. and Kuch, E.S., “Linear and Nonlinear Circuits”, McGraw-hill, New York, 1987.
- [5] Cirillo, M. and Pedersen, N.F., *On Bifurcation and transition to chaos in a Josephson junction*, Phys. Letter, 90 A(3) (1982), 150–152.
- [6] Cushman, R., *Periodic solutions of the autonomous Josephson equation*, in “Lecture Notes in Math.”, vol. 985, (1983), 319–326.
- [7] Davidson, A., Dueholm, B. and Beasley, M.R., *Experiments on intrinsic and they may included chaos in an RF-driven Josephson junction*, Phys. Rev. B., 33 (1986), 5127–5136.
- [8] D’Humieres, D., Beasley, M.R., Huberman, B.A. and Libchaber, A.F., *Chaotic states and routes to chaos in the forced pendulum*, Phys. Rev. A., 26(6) (1982), 3483–3492.
- [9] Graham, R. and Keymer, J., *Level repulsion in power spectra of chaotic Josephsonjunctions*, Phys. Rev. A., A(44) (1991), 6281–6291.
- [10] Graham, R., Schlantman, M. and Keymer, J., *Dynamical localization in Josephson junctions*, Phys. Rev. Lett., 67 (1991), 255–272.
- [11] Levi, M., Hoppensteadt, F. and Miranker, W., *Dynamics of the Josephson junction*, Quart, Appl. Math., 35 (1978), 167–198.
- [12] Li, G.X. and Moon, F.C., *Criteria for chaos of a three-well potential oscillator with homoclinic and heteroclinic orbits*, J. Sound and Vibrations, 136(1) (1990), 17–34.
- [13] Guckenheimer, J. and Holmes, P., “Nonlinear Oscillations, Dynamical Systems, and Bifurcations of Vector Fields,” Springer-Verlag, New York, 1983.
- [14] Lindsey, W.C., “Synchronization Systems In Communication And Control,” Prentice-Hall, New Jersey, 1972.
- [15] Levensen, M.T., *The chaotic oscilloscope*, Amer. J. Phys., 61 (1993), 155–193.
- [16] Jing, Zhu-Jun, *Application of qualitative methods of differential equations to study phase-locked loops*, SIAM J. Appl. Math., 43(6)(1983), 1749–1758.
- [17] Jing, zhu-Jun, *Chaotic behavior in the Josephson equations with periodic force*, SIAM J. Appl. Math., 49(6) (1989), 847–856.
- [18] Josephson, D., Phys. Lett., 1(1962), 251; Adv. Phys., 14 (1965), 419.
- [19] Kapitaniak, Thomas, “Chaotic Oscillators Theory and Applications,” World Scientific, Singapore, 1992.
- [20] Korsch, H.J. and Jodj, H.J., “Chaos-A Program Collection for the PC,” Springer-Verlag, 1994.
- [21] Moon, F.C., “Chaotic Vibrations: A Introduction For Applied Scientists And Engineers,” John Wiley, 1987.
- [22] Pai, M.A., Sauer, P.W., Lesieutre, B.C. and Adapa, R., *Structural stability in power systems-effect of load models*, IEEE Trans. on Power Systems, 10(02) (1995), 609–615.
- [23] Rasband, S.N., “Chaotic Dynamics of Nonlinear Systems,” Wiley, New York, 1990.
- [24] Sanders, J.A. and Verhulst, F., “Averaging Methods in Nonlinear Dynamical Systems”, Applied Mathematics Sciences, vol. 59, Springer-Verlag, New York, 1985.
- [25] Salam, F.M.A. and Satry, S., *Dynamics of the forced Josephson junction circuit: the regions of chaos*, IEEE Trans. Circuits and Systems, 32 (1985), 784–796.
- [26] Sanders, J.A. and Cushman, R.H., *Limit cycles in Josephson equation*, SIAM. J. Math. Anal., 17 (1986), 495–511.

- [27] Sanders, J.A., *The (Driven) Josephson equations: An exercise in asymptotics*, in Lecture Notes in Math., vol. 985, 288–318, (1983).
- [28] Schechter, S., *The saddle-node separatrix-loop bifurcation*, SIAM. J. Math. Anal., 18(4) (1987), 1142–1156.
- [29] Schechter, S., *Melnikov's method at a saddle-node and the dynamics of the forced Josephson junction*, SIAM. J. Math. Anal., 18(6) (1987), 1699–1715.
- [30] Szemplinska-Stupnicka, W, Iooss, G. and Moon, F.C., “Chaotic Motions in Nonlinear Dynamicalsystems,” Springer-Verlag, 1988.
- [31] Wiggins, S., “Introduction to Applied Nonlinear Dynamical Systems and Chaos,” Springer-Verlag, New York, 1990.
- [32] Yagasaki, K., *A simple feedback control system: Bifurcations of periodic orbits and chaos*, Nonlinear Dynamics, 9 (1996), 391–417.
- [33] Yagasaki, K., *Chaos in a pendulum with feedback control*, Nonlinear Dynamics, 6 (1994), 125–142.
- [34] Yeh, W.J. and Kao, Y.H., *Intermittence in Josephson junctions*, Appl. Phys. Lett., 42 (1983), 299–.

Received June 2000; revised December 2000.

*E-mail address:* jingzj@263.net